

Curvature Dependency of Surface Tension in Multicomponent Systems

Erik Santiso

Dept. of Chemical Engineering, North Carolina State University, Raleigh, NC 27695

Abbas Firoozabadi

Reservoir Engineering Research Institute, Palo Alto, CA 94306

DOI 10.1002/aic.10588

Published online September 1, 2005 in Wiley InterScience (www.interscience.wiley.com).

The effect of curvature on the surface tension of droplets and bubbles in both single and multicomponent systems is modeled using the basic equations from classical thermodynamics. The three expressions used in our work are the Gibbs adsorption equation for multicomponent systems, the relation between the surface tension at the surface of tension and the distance parameter δ , and the Macleod–Sugden equation for surface tension and its extension to multicomponent systems. The Peng–Robinson equation of state is used to describe the bulk phases. We also assume that the surface tension expression remains valid in terms of the properties of the bulk phases for both flat and curved interfaces. For a flat surface we have developed a rigorous thermodynamics approach for the calculation of the Tolman distance parameter. For curved surfaces, the results from our model reveal a decrease in surface tension with curvature in bubbles and a nonmonotonic behavior in droplets for single-component systems. Our predictions are in good agreement with the literature results when the interface is described using the framework of the density functional theory by three different groups. For multicomponent systems, the results show that the surface tension in a bubble, although monotonic with curvature, can increase or decrease in a large bubble depending on the temperature and composition of the mixture. In a droplet, the surface tension can have a nonmonotonic behavior similar to that of single-component systems. © 2005 American Institute of Chemical Engineers AIChE J, 52: 311–322, 2006

Keywords: curvature effect on multicomponents, surface tension, multicomponent mixtures

Introduction

Surface tension is a prime parameter in the basic formulation of a large number of processes including nucleation and cluster formation. The work of formation of a critical-size nucleus is proportional to the surface tension to the power three.¹ The

solute clustering in supersaturated solutions and concentration gradients in a vertical column of a supersaturated solution may also depend on the surface tension of nanoparticles.² In addition to applications in nucleation and solute clustering in supersaturated solutions, there is a wide interest in the important role of surface tension in determining the behavior of small droplets and bubbles including oil-recovery processes. For some time it has been recognized that when a cluster of a new phase is small (that is, has a high curvature), the surface tension is size dependent (that is, curvature dependent).

In an early paper, Tolman^{3,4} derived the expression for the

A. Firoozabadi is also affiliated with: Dept. of Chemical Engineering, Yale University, New Haven, CT 06520.

Correspondence concerning this article should be addressed to A. Firoozabadi at abbas.firoozabadi@yale.edu.

effect of droplet size on surface tension in a single-component system. A key parameter in Tolman's work is the parameter δ , the distance between the surface of tension and the equimolecular dividing surface. For a plane surface of separation, Tolman computed δ for a variety of substances, including water.³ His results show that the distance δ is positive and of the order of 1 to 3.5 Å (of the order of the intermolecular distances in liquids) for pure substances over the range of conditions studied.

Since the early work of Tolman, many investigators have studied the curvature dependency of surface tension and nucleation theory. There is generally consensus that the curvature dependency of surface tension may indeed result in significant variation of the work of formation of the critical nucleus⁵ and the nucleation rate.^{6,7} However, there is widespread confusion and controversy in the literature on the effect of curvature on the surface tension of a bubble and a droplet in single-component systems. Defay and Prigogine⁸ provide results for the effect of curvature on the surface tension of water at 18°C for both bubbles and droplets. Their results show an increase of the surface tension with increasing curvature for a bubble, whereas there is a decrease of surface tension with increasing curvature for a droplet (see Table 15.7 of Defay and Prigogine⁸). On the other hand, Kashchiev¹ presents results for water bubbles at 583 K and droplets at 293 K, both decreasing with increasing curvature (see Figure 6.1 of Kashchiev¹). Kashchiev used a positive value of δ of 1 Å for water droplets and bubbles.

Another example is the work of Hadjiagapiou,⁹ which provides results from density functional theory showing an increase of the surface tension for a droplet with increasing curvature, followed by a decrease at very high curvatures. Guermeur et al.¹⁰ also studied the effect of curvature on the surface tension for nitrogen bubbles and droplets. Their results show that the surface tension in the bubble decreases with increasing curvature. It has a nonmonotonic behavior in the droplet. On the other hand, as was stated earlier, many authors predict that the surface tension in, say, a droplet, should decrease rapidly with the radius (see, for example, Lee et al.,¹¹ and the references therein).

In a different approach, Schmelzer and Baidakov¹² argue that the Gibbs method for determining the reference states for the description of bulk properties of the critical nucleus does not give a correct description of the bulk properties of the critical clusters at high supersaturation. They postulate that at a nonequilibrium state, the chemical potentials of the interface and the ambient phase (in their terminology, this is, the bulk phase other than the cluster bulk phase) are the same. They make other postulations and obtain new expressions, including a new expression for the pressure difference between the cluster phase and the other bulk phase given by $p_\alpha - p_\beta = 2\sigma/R_+ + \rho_\alpha(\mu_\alpha - \mu_\beta)$, where p is the pressure, ρ is the density, μ is the chemical potential, σ is the surface tension, and R_+ is the radius of the critical cluster (or critical nucleus); α is the cluster phase, and β is the ambient phase. All pertain to a critical cluster. (These are nomenclature from Schmelzer and Baidakov¹²; later, we will use our own.) Obviously, the expression for $(p_\alpha - p_\beta)$ from Schmelzer and Baidakov¹² is different from the Laplace equation given by $p_\alpha - p_\beta = (2\sigma/R_+)$. When the work from Schmelzer and Baidakov¹² is used, the surface tension both for a bubble and for a droplet decrease with curvature and approach zero at the spinodal. For a droplet, first

there is a slight increase (not noticeable) followed by a decrease with curvature. The work of critical cluster also approaches zero at the spinodal. We will return to this point later.

Most of the work on curvature dependency of the surface tension is limited to single components. Schmelzer et al.⁵ developed an empirical relation for δ in multicomponent systems for a droplet. In a more recent work, Baidakov et al.¹³ use an approach based on the work of Schmelzer and Baidakov¹² to study the effect of curvature on surface tension in mixtures. The results show that similar to a single-component system, the surface tension vanishes at the spinodal for a two-component mixture. In this work, we present results to show that there are differences in surface tension curvature dependency of pure components and multicomponent systems.

The purpose of our work is to derive the expressions for the curvature dependency of the surface tension for bubbles and droplets in both single and multicomponent systems. The derivations are based on the general expressions from classical thermodynamics using the work of Gibbs. We use an equation of state to describe the bulk-gas and liquid-phase properties. Therefore, there is no need to make assumptions regarding compressibility and compositional effects.

In the following, we first derive basic thermodynamic relations for the curvature dependency of the surface tension using a new simple approach. Then we apply the derived expressions coupled with a surface tension model to obtain the basic expressions for bubbles and droplets in single-component systems. Next, the basic expressions in multicomponent systems, also for both bubbles and droplets, are obtained. We also provide numerical examples. At the end we make several concluding remarks.

Thermodynamic Relations for the Curvature Dependency of Surface Tension

The two fundamental expressions that form the basis of this work can be directly obtained from the basic postulates of thermodynamics and have been derived by Ono and Kondo.¹⁴ The first expression is the *Gibbs adsorption equation* that, for a multicomponent system with a spherical interface, can be written as¹⁴

$$d\sigma = -s^\sigma dT - \sum_{i=1}^c \Gamma_i d\mu_i^\sigma + \left[\frac{\partial \sigma}{\partial a} \right] da \quad (1)$$

In this expression, σ is the surface tension; s^σ is the entropy per unit area of the interface (the superscript σ denotes a surface property); Γ_i and μ_i^σ are, respectively, the number of moles per unit area and chemical potential of component i in the interface; c is the number of components; a is the radius of the interface; and $[\partial \sigma / \partial a]$ represents the change in the surface tension when the mathematical dividing surface between the two phases is displaced. The particular dividing surface for which $[\partial \sigma / \partial a] = 0$ is called the *surface of tension*. Throughout this work, all properties referred to the surface of tension are identified with the subscript s . The second key equation mentioned above relates the surface tension to the radius of the interface and can be written as¹⁴

$$\left(\frac{\partial \ln \sigma_s}{\partial \ln a_s}\right)_{T, x_j^\alpha} = 2 \left(\frac{\delta}{a_s}\right) \frac{1 + (\delta/a_s) + (1/3)(\delta/a_s)^2}{1 + 2(\delta/a_s)[1 + (\delta/a_s) + (1/3)(\delta/a_s)^2]} \quad (2)$$

Note that in the above equation, the derivative is taken along a path where the temperature and composition of the continuous bulk phase (that is, mole fraction of the components x_j^α) are held constant (we refer to the small bulk phase as the cluster phase in the work). The parameter δ is the distance between two dividing surfaces: one is the surface of tension and the other is the dividing surface, defined by

$$\sum_{i=1}^c \Gamma_i \tilde{v}_i^\alpha = 0 \quad (3)$$

where \tilde{v}_i^α is the partial molar volume of component i in the continuous bulk phase (denoted by the superscript α). Parameters and properties referred to the dividing surface defined by Eq. 3 will be identified by the subscript v . The parameter δ is given by

$$\delta = a_v - a_s \quad (4)$$

Note that the distance parameter defined above is not related to geometry and that the two radii are constant for a given bubble or a droplet. One of the most challenging tasks in the past has been the estimation of δ . Some authors have made calculations to show that δ for a flat interface is positive, some others suggest that it is negative, and there is a third group who estimate δ to be zero for a flat interface. The implication for δ being zero for a flat interface is that there is no adsorption at the interface. The δ parameter for a flat interface may also have different signs in a bubble and in a droplet (see Bartell¹⁵ and references therein). Our goal in this work is to find a suitable approach in predicting this parameter. To achieve this goal, we need to find a clearer relation between δ and other properties of the system.

The total volume of the two-phase system based on the dividing surface defined by Eq. 3 can be expressed as

$$V = V_v^\alpha + V_v^\beta = \sum_{i=1}^c N_{i,v}^\alpha \tilde{v}_i^\alpha + \sum_{i=1}^c N_{i,v}^\beta \tilde{v}_i^\beta \quad (5)$$

where N_i is the number of moles of component i . We have introduced the superscript β to identify the cluster phase. Using the mass balance of component i to eliminate $N_{i,v}^\alpha$ from Eq. 5 we obtain

$$V = \sum_{i=1}^c N_i \tilde{v}_i^\alpha + \sum_{i=1}^c N_{i,v}^\beta (\tilde{v}_i^\beta - \tilde{v}_i^\alpha) \quad (6)$$

In Eq. 6, we have used Eq. 3 to eliminate the amounts of adsorption at the interface. The total volume of the two-phase system based on the surface of tension leads to

$$V = \sum_{i=1}^c N_i \tilde{v}_i^\alpha + \sum_{i=1}^c N_{i,s}^\beta (\tilde{v}_i^\beta - \tilde{v}_i^\alpha) - A_s \sum_{i=1}^c \Gamma_{i,s} \tilde{v}_i^\alpha \quad (7)$$

In Eq. 7, A_s is the surface area of the interface. Equating the right-hand sides of Eqs. 6 and 7 and simplifying, we obtain

$$V_v^\beta - \sum_{i=1}^c N_{i,v}^\beta \tilde{v}_i^\alpha = V_s^\beta - \sum_{i=1}^c N_{i,s}^\beta \tilde{v}_i^\alpha - A_s \sum_{i=1}^c \Gamma_{i,s} \tilde{v}_i^\alpha \quad (8)$$

By introducing the molar concentrations (that is, $c_i^\beta = N_{i,v}^\beta / V_v^\beta = N_{i,s}^\beta / V_s^\beta$) and rearranging we obtain

$$V_v^\beta = V_s^\beta - \frac{A_s \sum_{i=1}^c \Gamma_{i,s} \tilde{v}_i^\alpha}{1 - \sum_{i=1}^c c_i^\beta \tilde{v}_i^\alpha} \quad (9)$$

The equation above provides a relationship between the sizes of the cluster calculated for the two dividing surfaces. It also reveals that when there is adsorption the distance parameter may not be zero for a flat interface. One can write Eq. 9 in terms of the radii as

$$a_v = a_s^{2/3} \left(a_s - \frac{3 \sum_{i=1}^c \Gamma_{i,s} \tilde{v}_i^\alpha}{1 - \sum_{i=1}^c c_i^\beta \tilde{v}_i^\alpha} \right)^{1/3} \quad (10)$$

By combining Eqs. 4 and 10 we obtain

$$\frac{\delta}{a_s} = \left(1 - \frac{3 \sum_{i=1}^c \Gamma_{i,s} \tilde{v}_i^\alpha}{a_s (1 - \sum_{i=1}^c c_i^\beta \tilde{v}_i^\alpha)} \right)^{1/3} - 1 \quad (11)$$

which provides δ . To study the curvature dependency of the surface tension, one may rearrange Eq. 11 to

$$\delta \left[\frac{1}{3} \left(\frac{\delta}{a_s} \right)^2 + \frac{\delta}{a_s} + 1 \right] = \frac{-\sum_{i=1}^c \Gamma_{i,s} \tilde{v}_i^\alpha}{1 - \sum_{i=1}^c c_i^\beta \tilde{v}_i^\alpha} \quad (12)$$

Equation 12 relates δ to the properties of the two bulk phases and the interface for a multicomponent system. For a single-component system, Eq. 12 simplifies to

$$\delta \left[\frac{1}{3} \left(\frac{\delta}{a_s} \right)^2 + \frac{\delta}{a_s} + 1 \right] = \frac{\Gamma_s}{\rho^\beta - \rho^\alpha} \quad (13)$$

where ρ is the molar density (in this work we use the notation c_i for the molar density of component in a mixture and ρ as the molar density of a single-component fluid). Tolman⁴ derived Eq. 13 using an integral approach; we use the relationships from classical thermodynamics in our derivation. Note that one may not use Eq. 13 to generalize it to multicomponent mixtures without certain assumptions.⁵ By substituting Eq. 12 into Eq. 2 we find an equation for the curvature dependency of the surface tension that does not include δ :

$$\left(\frac{\partial \ln \sigma_s}{\partial \ln a_s}\right) = \frac{2 \sum_{i=1}^c \Gamma_{i,s} \tilde{v}_i^\alpha}{2 \sum_{i=1}^c \Gamma_{i,s} \tilde{v}_i^\alpha - a_s (1 - \sum_{i=1}^c c_i^\beta \tilde{v}_i^\alpha)} \quad (14)$$

Note that in the above equation the problem has shifted from obtaining the parameter δ to obtaining the amounts of adsorption of the components at the interface. To proceed further, we relate the surface tension to the properties of both bulk phases to obtain the sum that includes the amounts of adsorption.

The sum in Eq. 14 that contains the amounts of adsorption can be related to the surface tension by combining Gibbs adsorption equation and the chemical equilibrium conditions. By writing Eq. 1 for the surface of tension and replacing the surface chemical potentials by the chemical potentials in the bulk continuous phase we obtain

$$d\sigma_s = -s_s^\sigma dT - \sum_{i=1}^c \Gamma_{s,i} d\mu_i^\alpha \quad (15)$$

The differential of the chemical potentials of the continuous bulk phase can be expressed as

$$d\mu_i^\alpha = -\tilde{s}_i^\alpha dT + \tilde{v}_i^\alpha dP^\alpha + \sum_{j=1}^{c-1} \left(\frac{\partial \mu_i^\alpha}{\partial x_j^\alpha} \right)_{T, P^\alpha, x_{k \neq j, c}^\alpha} dx_j^\alpha \quad i = 1, \dots, c \quad (16)$$

Substituting Eq. 16 into Eq. 15 leads to

$$\left(\frac{\partial \sigma_s}{\partial P^\alpha} \right)_{T, x_i^\alpha} = - \sum_{i=1}^c \Gamma_{i,s} \tilde{v}_i^\alpha \quad (17)$$

Equation 17 is the sought relationship. Providing a model for the surface tension as a function of the properties of the two bulk phases, Eqs. 14 and 18 can be combined to evaluate the curvature dependency of the surface tension. In the following two sections we will present the methodology first for single-component and then for multicomponent systems.

Single-Component Systems

For a single-component system, Eq. 14 simplifies to

$$\left(\frac{\partial \ln \sigma_s}{\partial \ln a_s} \right) = \frac{2\Gamma_s}{2\Gamma_s - a_s(\rho^\alpha - \rho^\beta)} \quad (18)$$

Also, Eq. 17 becomes

$$\left(\frac{\partial \sigma_s}{\partial P^\alpha} \right)_T = \frac{-\Gamma_s}{\rho_s} \quad (19)$$

To proceed further we desire an equation for the equilibrium surface tension. For a single-component system, the well-known Macleod–Sugden equation for the surface tension^{16–18} of a flat interface can be used:

$$\sigma_\infty^{1/4} = \Pi(\rho^L - \rho^V) \quad (20)$$

In Eq. 20, σ_∞ is the surface tension of the flat interface, Π is the parachor, and the superscripts L and V denote liquid and vapor, respectively. Equation 20 provides the surface tension of non-polar fluids with a remarkable accuracy over a wide range of temperature conditions¹⁹ and, although it was introduced empirically,^{16,17} it was later derived theoretically.¹⁸ In what follows we will use two different approaches: with respect to Eq. 20, we assume that (1) the expression is valid for large values of the interface radius and obtain the limiting dependency of δ for a flat interface (that is, δ_∞); then assume that δ is constant to obtain the curvature dependency of the surface tension; and (2) the expression applies to a surface with a curved interface, which implies that δ can change with curvature. The assumptions have to be examined for their validity. Let us use the terms “ δ_∞ model” and “ Π model” to refer to the two methods.

It turns out that in either approach it will be necessary to obtain δ as a function of curvature assuming that Eq. 20 is valid for a curved interface. For the δ_∞ model we will take the limit as the interface radius tends to infinity. Thus, we will replace σ_∞ by σ_s in Eq. 20. Let us first consider a bubble in a continuous bulk liquid phase and replace L and V in Eq. 20 by α and β , respectively. The expression for surface tension will take the form

$$\sigma_s^{1/4} = \Pi(\rho^\alpha - \rho^\beta) \quad (21)$$

The droplet in a continuous bulk vapor phase will be considered later. By substituting Eq. 21 into Eq. 19 we obtain

$$\Gamma_s = 4\Pi\rho^\alpha\sigma_s^{3/4} \left[\left(\frac{\partial \rho^\beta}{\partial P^\alpha} \right)_T - \left(\frac{\partial \rho^\alpha}{\partial P^\alpha} \right)_T \right] \quad (22)$$

The second derivative in the square brackets in Eq. 22 is given by

$$\left(\frac{\partial \rho^\alpha}{\partial P^\alpha} \right)_T = \rho^\alpha C_T^\alpha \quad (23)$$

where C_T^α is the isothermal compressibility of phase α , which can be readily obtained from an equation of state. Next we find an expression for the first derivative in Eq. 22. From the chain rule we write

$$\left(\frac{\partial \rho^\beta}{\partial P^\alpha} \right)_T = \left(\frac{\partial \rho^\beta}{\partial P^\beta} \right)_T \left(\frac{\partial P^\beta}{\partial P^\alpha} \right)_T = \rho^\beta C_T^\beta \left(\frac{\partial P^\beta}{\partial P^\alpha} \right)_T \quad (24)$$

The derivatives in Eq. 24 are taken along an equilibrium path. Therefore, we can write

$$\left(\frac{\partial \mu^\alpha}{\partial P^\alpha} \right)_T = \left(\frac{\partial \mu^\beta}{\partial P^\alpha} \right)_T = \left(\frac{\partial \mu^\beta}{\partial P^\beta} \right)_T \left(\frac{\partial P^\beta}{\partial P^\alpha} \right)_T \quad (25)$$

Replacing the derivatives of the chemical potentials with respect to the pressure of their respective phases by the inverse of the molar densities, we obtain

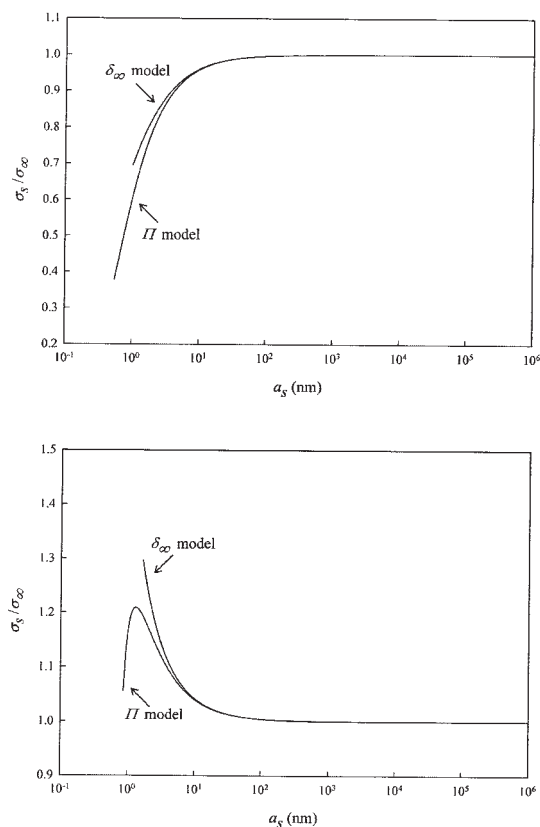


Figure 1. Curvature dependency of the surface tension in *n*-pentane at 310.9 K from the δ_∞ and Π models.

(a) Bubble, (b) droplet.

$$\left(\frac{\partial P^\beta}{\partial P^\alpha} \right)_T = \left(\frac{\rho^\beta}{\rho^\alpha} \right) \quad (26)$$

By combining Eqs. 22, 23, 24, and 26 we get

$$\Gamma_s = 4\Pi\sigma_s^{3/4} \left[(\rho^\beta)^2 C_T^\beta - (\rho^\alpha)^2 C_T^\alpha \right] \quad (27)$$

Equations 21 and 27, together with an equation of state, allow us to calculate the amount of adsorption at the surface of tension. For the δ_∞ model, we will use Eq. 27 to obtain the limiting value of δ as the radius of the interface goes to infinity. By substituting Eq. 27 into Eq. 13 and taking the limit as $a_s \rightarrow \infty$ we obtain

$$\delta_\infty = 4\Pi\sigma_s^{3/4} \frac{(\rho^\beta)^2 C_T^\beta - (\rho^\alpha)^2 C_T^\alpha}{\rho^\beta - \rho^\alpha} \quad (28)$$

Using δ_∞ as the constant value of δ we numerically integrate Eq. 2 and calculate the variation of σ_s with curvature. For the Π model, we will substitute Eq. 27 into Eq. 18 to get

$$\left(\frac{\partial \ln \sigma_s}{\partial \ln a_s} \right) = \frac{8\Pi\sigma_s^{3/4}[(\rho^\beta)^2 C_T^\beta - (\rho^\alpha)^2 C_T^\alpha]}{8\Pi\sigma_s^{3/4}[(\rho^\beta)^2 C_T^\beta - (\rho^\alpha)^2 C_T^\alpha] - a_s(\rho^\alpha - \rho^\beta)} \quad (29)$$

Equation 29 can be integrated numerically to compute the curvature dependency of the surface tension. In Figure 1a we show the surface tension σ_s as a function of the radius of the surface of tension for a bubble of *n*-pentane at 310.9 K using the two models. The Peng–Robinson equation of state²⁰ and the standard fourth-order Runge–Kutta method were used for calculations in Figure 1 and similar calculations to be presented later. The parachor of *n*-pentane was taken as 230. From this graph we note that: (1) the surface tension is constant down to $a_s \approx 100$ nm, and (2) the Π model predicts a sharper variation of the surface tension with curvature for $a_s < 10$ nm; the difference between the two models increases as the radius decreases. Figure 2a shows the variation of δ with curvature as predicted by the Π model. In this figure, it is also clear that there is almost no difference between the two models for sizes down to $a_s \approx 10$ nm, but as the radius decreases further, δ grows sharply, which accounts for the steeper variation of the surface tension predicted by this model at larger curvatures. This change in δ can be explained by the fact that the pressure, and thus the densities, starts to change much faster at these large curvatures. Granasy²¹ provides results similar to Figure

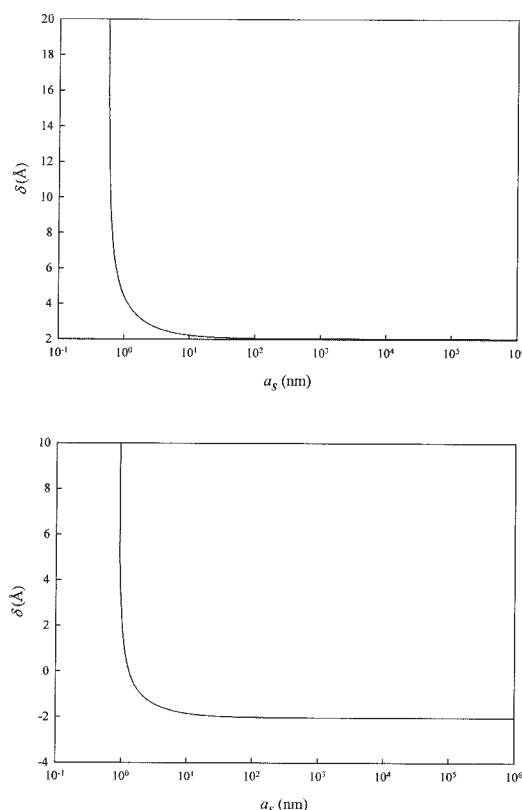


Figure 2. Curvature dependency of the parameter δ in *n*-pentane at 310.9 K from the Π model.

(a) Bubble, (b) droplet.

2a based on the semiempirical van der Waals/Cahn–Hilliard theory. Note that δ vs. the radius is positive in Figure 2a.

For a droplet in a continuous vapor phase, it is necessary to exchange the superscripts α and β in Eq. 21. Repeating the procedure we used for a bubble we obtain, for the limiting value of δ for a flat interface,

$$\delta_{\infty} = 4\Pi\sigma_{\infty}^{3/4} \frac{(\rho^{\alpha})^2 C_T^{\alpha} - (\rho^{\beta})^2 C_T^{\beta}}{\rho^{\beta} - \rho^{\alpha}} \quad (30)$$

Note that the above expression for δ_{∞} in a droplet is different from the expression derived in Bartell.¹⁵ There is no need to assume that density or volume can be expanded linearly with pressure. There is also no need for other assumptions except a need for a general expression for σ_{∞} . According to Eq. 30, even when $C_T^{\alpha} = 0$, δ_{∞} may not be zero. Substituting δ_{∞} from Eq. 30 into Eq. 2 and integrating, we obtain the variation of σ_{∞} with curvature for the δ_{∞} model.

For the constant Π model, we obtain

$$\left(\frac{\partial \ln \sigma_s}{\partial \ln a_s} \right) = \frac{8\Pi\sigma_s^{3/4}[(\rho^{\alpha})^2 C_T^{\alpha} - (\rho^{\beta})^2 C_T^{\beta}]}{8\Pi\sigma_s^{3/4}[(\rho^{\alpha})^2 C_T^{\alpha} - (\rho^{\beta})^2 C_T^{\beta}] - a_s(\rho^{\alpha} - \rho^{\beta})} \quad (31)$$

Figure 1b shows the variation of the surface tension with the radius of the surface of tension using the two models for a droplet of *n*-pentane at 310.9 K. For a droplet, the difference between the δ_{∞} model and the Π model is more pronounced: for the δ_{∞} model, the surface tension increases monotonically with decreasing radius whereas the Π model predicts that the surface tension will go through a maximum at an approximate radius of 1.1 nm and then decreases rapidly with decreasing radius. Hadjiagapiou⁹ and Guermeur et al.¹⁰ predicted a similar nonmonotonic behavior. Figure 2b shows the variation of δ with curvature as predicted by the Π model, where the variation of δ with curvature is similar to that of the bubble, being almost constant at small curvatures and then growing fast as the radius decreases. However, δ_{∞} is negative for the droplet and δ changes sign and causes the surface tension to go through a maximum. A negative value for δ_{∞} in a droplet has been presented in Bartell¹⁵ and Granasy²¹ using different approaches.

In Bartell,¹⁵ δ_{∞} is approximated by $-C_T^{\alpha}\sigma_{\infty}/3$, based on a number of assumptions. Based on another set of assumptions Laaksonen and McGraw⁶ obtained $\delta_{\infty} \approx -C_T^{\alpha}\sigma_{\infty}$. Granasy²¹ discusses the difference between the density function (DF) approach in predicting a negative δ_{∞} and the molecular dynamics (MD) simulations, which predict a positive δ_{∞} for a droplet. According to the definition of distance parameter in Eq. 4, there is only consistency when δ_{∞} from bubbles and droplets have the same magnitude but different sign. Both imply that the equimolecular dividing surface is closer to the bulk liquid phase than the surface of tension. In other words, the change in sign is explained by the fact that in the bubble the distances are measured from the gas side and in a droplet they are measured from the liquid side. However, for a multicomponent system, this is not the case as expected (as we will show later).

The results shown above for the curvature dependency of surface tension in bubbles and droplets have similar trends to those of Hadjiagapiou⁹ and Guermeur et al.¹⁰ Figure 3a shows

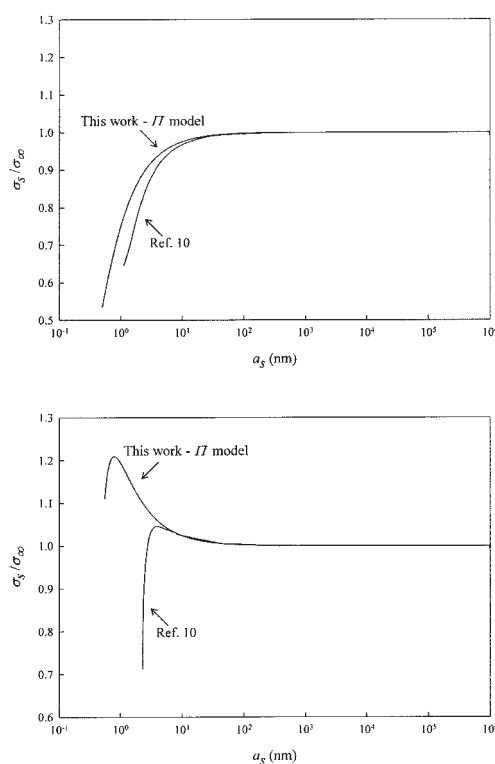


Figure 3. Curvature dependency of the surface tension in nitrogen at 77.3 K from the Π model and from Guermeur et al.¹⁰

(a) Bubble, (b) droplet.

a comparison between the results of Guermeur et al. for bubbles of nitrogen at 77.3 K and the results for the same system obtained with our Π model (nitrogen parachor of 52 was used in our calculations based on surface tension data for nitrogen). Figure 3b shows the same comparison for a droplet of nitrogen at the same temperature. In both figures we observe that the trends predicted by our model and the work of Guermeur et al. are the same, although the two models are very different. Guermeur et al. describe the inhomogeneous fluid in the interface using a stress tensor in the framework of gradient theory, and predict a sharper variation of the surface tension with curvature for the bubbles and a smaller variation for the droplets. Although they also obtain a maximum in the surface tension plot for the droplet, the maximum is at a smaller curvature and the corresponding surface tension is also smaller. The results for our δ_{∞} model (not shown) are farther from their results in both cases.

To compare with Hadjiagapiou's results, we computed the surface tension as a function of curvature for a droplet of argon at a reduced temperature of 0.8 (argon parachor of 52 was used in our calculations). Argon was chosen for comparison because it is a substance well suited for Hadjiagapiou's treatment of thermodynamic properties. The results, in terms of the reduced variables defined in his work, are shown in Figure 4. In this case, our Π model predicts a smaller variation of the surface tension with curvature than Hadjiagapiou's model, although our Π model predicts a smaller droplet radius for the maximum

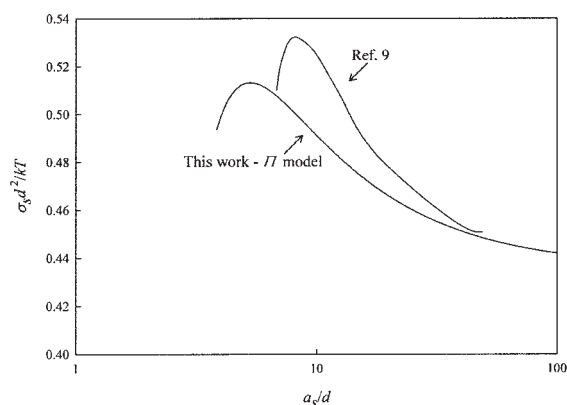


Figure 4. Curvature dependency of the surface tension in Argon at a reduced temperature of 0.8 from the II model and from Hadjiagapiou.⁹

The new variables appearing in the dimensionless groups plotted are d (molecular diameter) and k (Boltzmann's constant).

surface tension. In view of the simplicity of our model, it is interesting to note that its predictions are close to those of Hadjiagapiou, which is based on density functional theory.

Before proceeding to multicomponent systems, we must point out a deficiency with respect to the work of critical cluster formation at the spinodal (that is, at the limit of stability). The work of critical cluster formation is expected to vanish as we approach the spinodal. In the classical theory of nucleation, the barrier height approaches a finite value at the spinodal, which is not correct.²² When one accounts for the effect of curvature on the surface tension, the work of critical cluster formation at the spinodal reduces, but may not vanish. This is to be expected because of the extremely small size of the clusters, constituting say some 40 atoms, at the spinodal. Instead of using classical thermodynamics, one may use statistical or molecular thermodynamics for very small clusters (that is, at very high supersaturation) to account for nonclassical effects.²² In our approach, similar to that of Guermeur et al.,¹⁰ the surface tension for a droplet is greater than the flat interface for large droplets but becomes smaller for smaller droplets. For bubbles, the surface tension remains less than σ_∞ . These results are consistent with the work of Oxtoby and Evans,²² that classical and nonclassical barrier heights cross from droplet formation but do not for bubble formation.

Schmelzer and coworkers, in a different approach, as we stated earlier, use certain postulations that lead to the vanishing of the work of critical cluster formation as well as the vanishing of the surface tension at the spinodal (Schmelzer and Baidakov¹² and references within).

Figure 5 shows the plot for the work of critical cluster formation (in dimensionless units) vs. a_s in a bubble of n -pentane at 310.9 K. Note that as the spinodal is approached, W/kT decreases. Despite a small W of about $1.5kT$, it does not vanish at the spinodal. The droplet also has a similar behavior. The work of critical cluster formation for the Argone bubble at the spinodal (for $T_r = 0.8$) is about $2.5kT$, which is not far from kT .

Multicomponent Systems

For multicomponent systems we follow an approach similar to that of single-component systems. Weinaug and Katz have extended Eq. 20 to multicomponent systems^{23,24}:

$$\sigma_\infty^{1/4} = \sum_{i=1}^c \Pi_i (c_i^L - c_i^V) \quad (32)$$

The above equation provides good predictions in nonpolar multicomponent hydrocarbon mixtures.^{23,24} To apply Eq. 32 to obtain the curvature dependency of the surface tension, we will follow an approach similar to the one used in the previous section. Again, we will explore two options: (1) assume that Eq. 32 is valid for curved interfaces with a very large radius, use it to obtain the limiting value δ_∞ for the flat interface, and then use δ_∞ to integrate Eq. 2; and (2) assume that Eq. 32 is valid for a curved interface, thus allowing for δ to vary with curvature. To keep the terminology used in previous section, we will call the first approach the “ δ_∞ model” and the second the “II model.”

Similar to a single-component system, we need to find an expression for δ as a function of curvature assuming that Eq. 32 is valid for a curved interface. For the δ_∞ model we will take the flat interface limit in the resulting expression. Thus, we will replace σ_∞ by σ_s in Eq. 32. First we will consider a bubble in a continuous bulk liquid phase and replace L and V in Eq. 20 by α and β , respectively. With the altered notation, Eq. 32 takes the form

$$\sigma_s^{1/4} = \sum_{i=1}^c \Pi_i (c_i^\alpha - c_i^\beta) \quad (33)$$

Substituting Eq. 33 into Eq. 17 leads to

$$\sum_{i=1}^c \Gamma_{i,s} \tilde{v}_i^\alpha = 4\sigma_s^{3/4} \sum_{i=1}^c \Pi_i \left[\left(\frac{\partial c_i^\beta}{\partial P^\alpha} \right)_{T,x_j^\alpha} - \left(\frac{\partial c_i^\alpha}{\partial P^\alpha} \right)_{T,x_j^\alpha} \right] \quad (34)$$

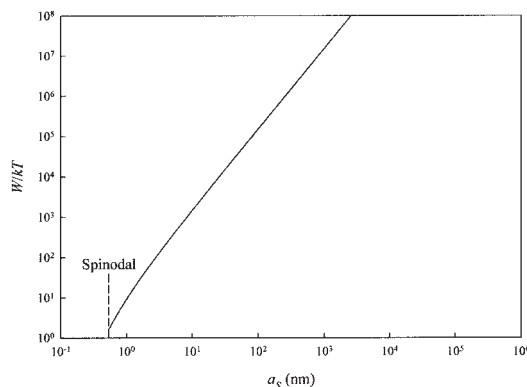


Figure 5. Work of cluster formation (critical) vs. radius of the surface of tension in the n -pentane bubble at $T = 310.9$ K.

As in Eq. 22, the second derivative inside the square brackets in Eq. 34 can be readily obtained from an equation of state:

$$\left(\frac{\partial c_i^\alpha}{\partial P^\alpha}\right)_{T,x_j^\alpha} = C_T^\beta c_i^\alpha \quad i = 1, \dots, c \quad (35)$$

The first derivative, however, is more complicated to evaluate. Let us write the differential of the variable c_i^β in two different ways: first as a function of the variables of phase β and then as a function of the variables of phase α

$$dc_i^\beta = \left(\frac{\partial c_i^\beta}{\partial T}\right)_{P^\beta, x_j^\beta} dT + \left(\frac{\partial c_i^\beta}{\partial P^\beta}\right)_{T, x_j^\beta} dP^\beta + \sum_{j=1}^{c-1} \left(\frac{\partial c_i^\beta}{\partial x_j^\beta}\right)_{T, P^\beta, x_{k \neq j}^\beta} dx_j^\beta \quad i = 1, \dots, c \quad (36)$$

$$dc_i^\beta = \left(\frac{\partial c_i^\beta}{\partial T}\right)_{P^\alpha, x_j^\alpha} dT + \left(\frac{\partial c_i^\beta}{\partial P^\alpha}\right)_{T, x_j^\alpha} dP^\alpha + \sum_{j=1}^{c-1} \left(\frac{\partial c_i^\beta}{\partial x_j^\alpha}\right)_{T, P^\alpha, x_{k \neq j}^\alpha} dx_j^\alpha \quad i = 1, \dots, c \quad (37)$$

Considering a process at constant temperature and composition of the phase α , which are the conditions for which Eq. 2 holds, and equating Eqs. 36 and 37 and writing the result in terms of the derivatives with respect to P^α

$$\left(\frac{\partial c_i^\beta}{\partial P^\alpha}\right)_{T, x_j^\alpha} = \left(\frac{\partial c_i^\beta}{\partial P^\beta}\right)_{T, x_j^\beta} \left(\frac{\partial P^\beta}{\partial P^\alpha}\right)_{T, x_j^\alpha} + \sum_{j=1}^{c-1} \left(\frac{\partial x_j^\beta}{\partial P^\alpha}\right)_{T, x_j^\alpha} \left(\frac{\partial c_i^\beta}{\partial x_j^\beta}\right)_{T, P^\beta, x_{k \neq j}^\beta} \quad i = 1, \dots, c \quad (38)$$

Half of the derivatives in the right-hand side of Eq. 38 can be directly obtained from an equation of state

$$\left(\frac{\partial c_i^\beta}{\partial P^\beta}\right)_{T, x_j^\beta} = C_T^\beta c_i^\beta \quad i = 1, \dots, c \quad (39)$$

$$\left(\frac{\partial c_i^\beta}{\partial x_j^\beta}\right)_{T, P^\beta, x_{k \neq j}^\beta} = \rho^\beta [\delta_{ij} - \delta_{ic} + c_i^\beta (\tilde{v}_j^\beta - \tilde{v}_c^\beta)] \quad i = 1, \dots, c \quad j = 1, \dots, c-1 \quad (40)$$

Equation 40 is obtained from the definition of $c_i^\beta = x_i^\beta \rho^\beta$ and the Gibbs–Duhem equation in terms of partial molar volumes (see problem 1.5 of Chapter I in Firoozabadi²⁵). The symbol δ in Eq. 40 is the Kronecker delta. By substituting Eqs. 39 and 40 into Eq. 38 we obtain

$$\left(\frac{\partial c_i^\beta}{\partial P^\alpha}\right)_{T, x_j^\alpha} = C_T^\beta c_i^\beta \left(\frac{\partial P^\beta}{\partial P^\alpha}\right)_{T, x_j^\alpha} + \rho^\beta \left(\frac{\partial x_i^\beta}{\partial P^\alpha}\right)_{T, x_j^\alpha} + \rho^\beta c_i^\beta \sum_{j=1}^{c-1} (\tilde{v}_c^\beta - \tilde{v}_j^\beta) \left(\frac{\partial x_j^\beta}{\partial P^\alpha}\right)_{T, x_j^\alpha} \quad i = 1, \dots, c-1 \quad (41)$$

And, for $i = c$

$$\left(\frac{\partial c_i^\beta}{\partial P^\alpha}\right)_{T, x_j^\alpha} = \beta^\beta c_i^\beta \left(\frac{\partial P^\beta}{\partial P^\alpha}\right)_{T, x_j^\alpha} - \rho^\beta \sum_{j=1}^{c-1} \left(\frac{\partial x_j^\beta}{\partial P^\alpha}\right)_{T, x_j^\alpha} + \rho^\beta c_i^\beta \sum_{j=1}^{c-1} (\tilde{v}_c^\beta - \tilde{v}_j^\beta) \left(\frac{\partial x_j^\beta}{\partial P^\alpha}\right)_{T, x_j^\alpha} \quad (42)$$

However, from the sum condition of phase β

$$\sum_{j=1}^{c-1} \left(\frac{\partial x_j^\beta}{\partial P^\alpha}\right)_{T, x_j^\alpha} = - \left(\frac{\partial x_c^\beta}{\partial P^\alpha}\right)_{T, x_j^\alpha} \quad (43)$$

By substituting Eq. 43 into Eq. 42 we obtain Eq. 41 with $i = c$. Thus, we can regard Eq. 41 as valid for all $i = 1, \dots, c$. To use Eq. 41 we need to find the derivatives of the pressure and composition of phase β with respect to the pressure of phase α . We use an approach similar to the one used for the single-component system. Because the derivatives appearing in Eq. 41 are taken in an equilibrium path, we use

$$\mu_i^\alpha = \mu_i^\beta \quad i = 1, \dots, c \quad (44)$$

Differentiating Eq. 44 with respect to the pressure of phase α at constant temperature and composition of phase α we obtain

$$\left(\frac{\partial \mu_i^\alpha}{\partial P^\alpha}\right)_{T, x_j^\alpha} = \left(\frac{\partial \mu_i^\beta}{\partial P^\alpha}\right)_{T, x_j^\alpha} \quad i = 1, \dots, c \quad (45)$$

The derivative on the left-hand side of Eq. 45 is the partial molar volume of component i in phase α . For the derivative in the right hand-side, one can write

$$\left(\frac{\partial \mu_i^\beta}{\partial P^\alpha}\right)_{T, x_j^\alpha} = \left(\frac{\partial \mu_i^\beta}{\partial P^\beta}\right)_{T, x_j^\beta} \left(\frac{\partial P^\beta}{\partial P^\alpha}\right)_{T, x_j^\alpha} + \sum_{j=1}^{c-1} \left(\frac{\partial x_j^\beta}{\partial P^\alpha}\right)_{T, x_j^\alpha} \left(\frac{\partial \mu_i^\beta}{\partial x_j^\beta}\right)_{T, P^\beta, x_{k \neq j}^\beta} \quad i = 1, \dots, c \quad (46)$$

The first derivative on the right-hand side is the partial molar volume of component i in phase β . By substituting Eq. 46 into Eq. 45 we obtain

$$\tilde{v}_i^\alpha = \tilde{v}_i^\beta \left(\frac{\partial P^\beta}{\partial P^\alpha} \right)_{T, x_j^\alpha} + \sum_{j=1}^{c-1} \left(\frac{\partial x_j^\beta}{\partial P^\alpha} \right)_{T, x_j^\alpha} \left(\frac{\partial \mu_i^\beta}{\partial x_j^\beta} \right)_{T, P^\beta, x_{k \neq j, c}^\beta} \quad i = 1, \dots, c \quad (47)$$

Upon multiplying Eq. 47 by x_j^β and taking the sum we find

$$\sum_{j=1}^c x_j^\beta \tilde{v}_j^\alpha = v^\beta \left(\frac{\partial P^\beta}{\partial P^\alpha} \right)_{T, x_j^\alpha} + \sum_{k=1}^{c-1} \left(\frac{\partial x_k^\beta}{\partial P^\alpha} \right)_{T, x_j^\alpha} \sum_{j=1}^c x_j^\beta \left(\frac{\partial \mu_j^\beta}{\partial x_k^\beta} \right)_{T, P^\beta, x_{l \neq k, c}^\beta} \quad (48)$$

where v is the molar volume. From the Gibbs–Duhem equation for phase β

$$\sum_{j=1}^c x_j^\beta \left(\frac{\partial \mu_j^\beta}{\partial x_k^\beta} \right)_{T, P^\beta, x_{l \neq k, c}^\beta} = 0 \quad (49)$$

Combining Eqs. 48 and 49 provides

$$\left(\frac{\partial P^\beta}{\partial P^\alpha} \right)_{T, x_j^\alpha} = \rho^\beta \sum_{i=1}^c x_i^\beta \tilde{v}_i^\alpha = \sum_{i=1}^c c_i^\beta \tilde{v}_i^\alpha \quad (50)$$

Substitution of Eq. 50 into Eq. 47 leads to

$$\sum_{j=1}^{c-1} \left(\frac{\partial x_j^\beta}{\partial P^\alpha} \right)_{T, x_j^\alpha} \left(\frac{\partial \mu_i^\beta}{\partial x_j^\beta} \right)_{T, P^\beta, x_{k \neq j, c}^\beta} = \tilde{v}_i^\alpha - \tilde{v}_i^\beta \sum_{j=1}^c c_j^\beta \tilde{v}_j^\alpha \quad i = 1, \dots, c \quad (51)$$

Note that, although Eq. 51 is valid for $i = 1, \dots, c$, only $(c - 1)$ of the equations are independent because we already used their sum to obtain Eq. 50. The first $(c - 1)$ equations in Eq. 51 can be used to obtain the derivatives of the compositions of phase β with respect to the pressure of phase α , provided we use an equation of state to obtain the derivatives of the chemical potentials with respect to the compositions in phase β .

Substituting Eqs. 35, 41, and 50 into Eq. 34 yields

$$\delta_\infty^b = \frac{-4\sigma_s^{3/4} \sum_{i=1}^c \Pi_i \left[C_T^\beta c_i^\beta \sum_{j=1}^c c_j^\beta \tilde{v}_j^\alpha + \rho^\beta \left(\frac{\partial x_i^\beta}{\partial P^\alpha} \right)_{T, x_j^\alpha} - \rho^\beta c_i^\beta \sum_{j=1}^c \tilde{v}_j^\beta \left(\frac{\partial x_j^\beta}{\partial P^\alpha} \right)_{T, x_j^\alpha} - C_T^\alpha c_i^\alpha \right]}{1 - \sum_{i=1}^c c_i^\beta \tilde{v}_i^\alpha} \quad (53)$$

Note that the superscript b indicates the limiting value for the bubble. Unlike in single-component systems, in mixtures the dividing surface defined by Eq. 3 is different for different

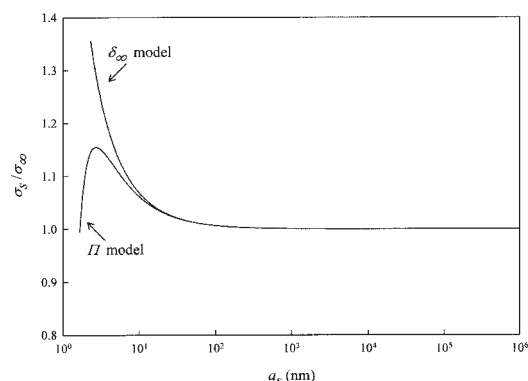
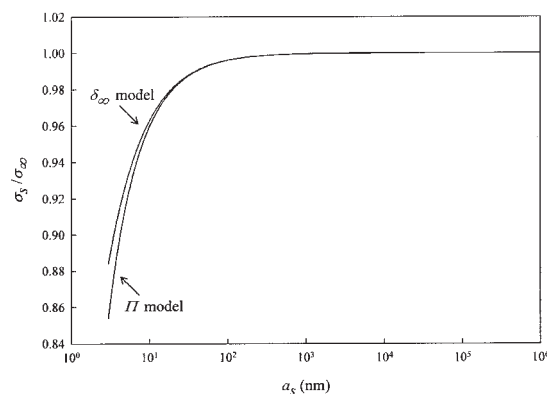


Figure 6. Curvature dependency of the surface tension in a binary mixture of propane and n -octane from the δ_∞ and Π models.

(a) For a bubble of equimolar liquid mixture at 300 K; (b) for a droplet of equimolar gaseous mixture at 400 K.

$$\sum_{i=1}^c \Gamma_{i,s} \tilde{v}_i^\alpha = -4\sigma_s^{3/4} \sum_{i=1}^c \Pi_i \left[C_T^\alpha c_i^\alpha - C_T^\beta c_i^\beta \sum_{j=1}^c c_j^\beta \tilde{v}_j^\alpha - \rho^\beta \left(\frac{\partial x_i^\beta}{\partial P^\alpha} \right)_{T, x_j^\alpha} + \rho^\beta c_i^\beta \sum_{j=1}^c \tilde{v}_j^\beta \left(\frac{\partial x_j^\beta}{\partial P^\alpha} \right)_{T, x_j^\alpha} \right] \quad (52)$$

where the derivatives of the composition of phase β are obtained by solving the system of Eq. 51. For the δ_∞ model we will substitute Eq. 52 into Eq. 12 and take the limit as $a_s \rightarrow \infty$ to obtain

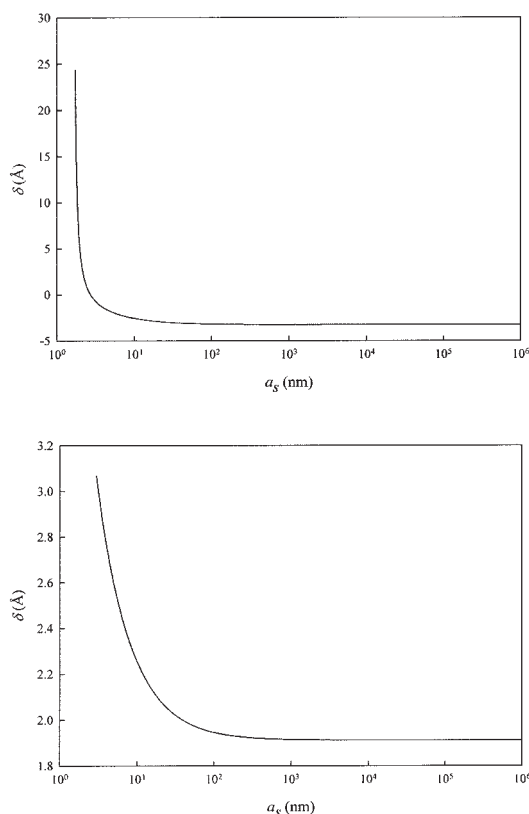


Figure 7. Curvature dependency of the parameter δ in a binary mixture of propane and *n*-octane from the II model.

(a) For a bubble of equimolar liquid mixture at 300 K; (b) for a droplet of equimolar gaseous mixture at 400 K.

obtained with the equations for a droplet not only in sign, but also in magnitude. To avoid ambiguity, in the discussion for multicomponent systems we will use the symbols δ_∞^b for the former and δ_∞^d for the latter. After substituting Eq. 53 into Eq. 2 and integrating we can calculate the curvature dependency of the surface tension. For the II model, Eq. 52 is substituted into Eq. 14 and the resulting equation is integrated numerically.

Figure 6a shows the variation of surface tension with the radius of the bubble in an equimolar liquid mixture of propane and *n*-octane at 300 K, using the δ_∞ and the II models. The parachors in the surface tension model are: C_3 , 150; nC_8 , 400. The binary interaction parameters in the Peng–Robinson equation of state were taken as zero. The behavior shown is similar to that obtained for the single-component system. The variation in surface tension is important only for bubble sizes of <10 nm. The overall change in surface tension in the two-component system considered is smaller than that in the single-component system. The variation of δ with curvature for the II model is shown in Figure 7a, which is consistent with the variation of the surface tension.

The equations for a droplet in a continuous bulk vapor phase can be obtained by exchanging the α and β superscripts in Eq. 33 and repeating the above procedure. In the following equations α will refer to the vapor phase and β to the liquid phase

$$\sum_{i=1}^c \Gamma_{i,s} \tilde{v}_i^\alpha = 4\sigma_s^{3/4} \sum_{i=1}^c \Pi_i \left[\beta^\alpha c_i^\alpha - \beta^\beta c_i^\beta \sum_{j=1}^c c_j^\beta \tilde{v}_j^\alpha - \rho^\beta \left(\frac{\partial x_i^\beta}{\partial P^\alpha} \right)_{T,x_i^\alpha} + \rho^\beta c_i^\beta \sum_{j=1}^c \tilde{v}_j^\beta \left(\frac{\partial x_j^\beta}{\partial P^\alpha} \right)_{T,x_j^\alpha} \right] \quad (54)$$

The derivatives of the composition in Eq. 54 will be found by solving the system of Eq. 51. For the limiting value of δ in a droplet

$$\delta_\infty^d = \frac{4\sigma_\infty^{3/4} \sum_{i=1}^c \Pi_i \left[C_T^\beta c_i^\beta \sum_{j=1}^c c_j^\beta \tilde{v}_j^\alpha + \rho^\beta \left(\frac{\partial x_i^\beta}{\partial P^\alpha} \right)_{T,x_i^\alpha} - \rho^\beta c_i^\beta \sum_{j=1}^c \tilde{v}_j^\beta \left(\frac{\partial x_j^\beta}{\partial P^\alpha} \right)_{T,x_j^\alpha} - C_T^\alpha c_i^\alpha \right]}{1 - \sum_{i=1}^c c_i^\beta \tilde{v}_i^\alpha} \quad (55)$$

A comparison of Eqs. 53 and 55 reveals the sign difference as well as the phase identity differences. For the δ_∞ model, we will substitute Eq. 55 into Eq. 2 and integrate to calculate the curvature dependency of the surface tension. For the II model, Eq. 54 is substituted into Eq. 14 and the result is integrated numerically.

Figure 6b shows the variation of the surface tension with the radius of the droplet in an equimolar gaseous mixture of propane and *n*-octane at 400 K. The same model as that of the bubble example was used. The behavior of the droplet in the multicomponent system is similar to that of the single-component droplet. Figure 7b, showing the variation of δ as a function of curvature, indicates a stronger increase of δ toward the high curvature region.

Figure 8 shows the behavior of the parameter δ_∞^b (taking the liquid as the continuous bulk phase) as a function of temperature for an equimolar liquid mixture of propane and *n*-octane. The

behavior is somewhat different from that observed in the single-component system; δ_∞^b becomes negative at temperatures closer to the critical point. This is an important new result, showing that the surface tension for the bubble can either increase or decrease with curvature depending on the temperature; this may be the case for a large bubble. In Figure 9 we show the effect of composition at different temperatures on the parameter δ_∞^b . At low temperatures and pressures, where the system can be regarded as ideal, δ_∞^b increases monotonically with composition of propane, growing from the value for pure *n*-octane to the value for pure propane. At higher temperatures, the curve first decreases and then increases with composition. As the temperature increases toward the critical point, the curve becomes monotonically decreasing and δ_∞^b for higher compositions of propane becomes negative. This shows that the surface tension increase or decrease with curvature de-

depends not only on the temperature but also on the composition of the mixture—the increase for a large bubble. As the system approaches the limit of stability (that is, the spinodal) the behavior changes.

We have carried out calculations for ternary systems; the behavior found is similar to that shown in Figures 6–9. Because the features are similar to what we obtained for the binaries, we have not included the results for the sake of brevity.

Concluding Remarks

We have derived the expressions for the Tolman distance parameter of a flat interface in both pure and multicomponent fluids. Based on physical interpretation, the distance parameter of a flat interface in a single-component system for a bubble should be positive and that of a droplet should be negative, both with the same absolute value. The models that predict the same sign are physically inconsistent.

A thermodynamic model is also presented for the effect of curvature on the surface tension in bubbles and droplets for both single and multicomponent systems. The results for the nonpolar hydrocarbon systems that we have studied reveal that:

(1) There is generally a decrease of surface tension in bubbles with increasing curvatures in single-component systems. The distance parameter δ for these systems is positive.

(2) For a droplet, if the distance parameter δ is assumed constant and equal to the value for the flat interface, there is an increase in the surface tension with increasing curvature in single-component systems. The distance parameter of the flat interface is generally negative. With a variable distance parameter model, the behavior of the surface tension is nonmonotonic; the surface tension increases with curvature first and then decreases. The predicted results from our thermodynamic model with a variable distance parameter are in qualitative agreement with the work of Hadjiagapiou⁹ and Guerneur et al.¹⁰ based on density functional theory. It is also in line with the work of Oxtoby and Evans.²²

(3) In multicomponent systems the distance parameter of the flat interface for a bubble may be either positive or negative depending on the temperature and composition. The surface

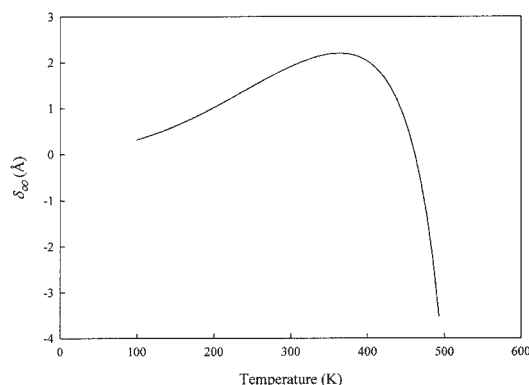


Figure 8. Parameter δ_{∞}^b vs. temperature for a bubble in an equimolar mixture of propane and *n*-octane.

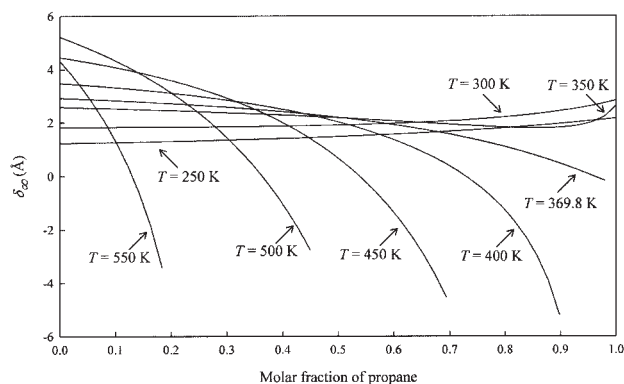


Figure 9. Parameter δ_{∞}^b vs. composition for a bubble in a liquid mixture of propane and *n*-octane at different temperatures.

tension may thus increase or decrease with curvature at different conditions for a large bubble.

(4) In both a bubble and in a droplet the surface of tension decreases for a small cluster(of molecules) from the Π model presented in the work. This is further evidence in support of the validity of the results from our Π model.

Acknowledgments

The work was supported by DOE DE-FC26-00BC15306, and member companies of Reservoir Engineering Research Institute.

Literature Cited

- Kashchiev D. *Nucleation: Basic Theory with Applications*. Oxford, UK: Butterworth-Heinemann; 2000.
- Larson MA, Garside J. Solute clustering and interfacial tension. *J Cryst Growth*. 1986;76:88-92.
- Tolman RC. The superficial density of matter at a liquid–vapor boundary. *J Chem Phys*. 1949;17:118-127.
- Tolman RC. The effect of droplet size on surface tension. *J Chem Phys*. 1949;17:333-337.
- Schmelzer JWP, Gutzow I, Schmelzer J. Curvature-dependent surface tension and nucleation theory. *J Colloid Interface Sci*. 1996;178:657-665.
- Laaksonen A, McGraw R. Thermodynamics, gas–liquid nucleation, and size-dependent surface tension. *Europhys Lett*. 1996;35:367-372.
- McGraw R, Laaksonen A. Interfacial curvature free energy, the Kelvin relation, and vapor–liquid nucleation. *J Chem Phys*. 1997;106:5284-5287.
- Defay R, Prigogine J. *Surface Tension and Adsorption*. London: Longman; 1966.
- Hadjiagapiou I. Density-functional theory for spherical drops. *J Phys Condens Matter*. 1994;6:5303-5322.
- Guerneur R, Biquard F, Jacolin C. Density profiles and surface-tension of spherical interfaces—Numerical results for nitrogen drops and bubbles. *J Chem Phys*. 1985;82:2040-2051.
- Lee DJ, Telo da Gama MMT, Gubbins KE. A microscopic theory for spherical interfaces—Liquid drops in the canonical ensemble. *J Chem Phys*. 1986;85:490-499.
- Schmelzer JWP, Baidakov VG. Kinetics of condensation and boiling: Comparison of different approaches. *J Phys Chem B*. 2001;105:11595-11604.
- Baidakov VG, Boltashev GS, Schmelzer JWP. Comparison of different approaches to the determination of the work of critical cluster formation. *J Colloid Interface Sci*. 2000;231:312-321.
- Ono S, Kondo S. *Encyclopedia of Physics*. Flügge S, ed. Vol. 10. Berlin: Springer-Verlag; 1960:134.
- Bartell LS. Tolman's delta, surface curvature, compressibility effects, and the free energy of drops. *J Phys Chem B*. 2001;105:11615-11618.
- Macleod DB. Relation between surface tension and density. *Trans Faraday Soc*. 1923;19:38-42.

17. Sugden S. The variation of surface tension with temperature and some related functions. *J Chem Soc.* 1924;125:1177.
18. Fowler RH. A tentative statistical theory of Macleod's equation for surface tension and the parachors. *R Soc Lond Ser A Phys Sci.* 1937:229-246.
19. Poling BE, Prausnitz JM, O'Connell JP. *The Properties of Gases and Liquids*. 5th Edition. New York, NY: McGraw-Hill; 2001.
20. Peng DY, Robinson DB. New two-constant equation of state. *Ind Eng Chem Fundam.* 1976;15:59-64.
21. Granasy L. Semiempirical van der Waals/Cahn-Hilliard theory: Size dependence of the Tolman length. *J Chem Phys.* 1998;109:9660-9663.
22. Oxtoby DW, Evans R. Nonclassical nucleation theory for the gas-liquid transition. *J Chem Phys.* 1988;89:7521-7530.
23. Weinaug CF, Katz DL. Surface tensions of methane-propane mixtures. *Ind Eng Chem.* 1943;35:239.
24. Firoozabadi A, Katz DL, Soroosh H, Sajjadian VA. Surface tension of reservoir crude oil-gas systems recognizing the asphalt in the heavy fraction. *SPE Reservoir Eng.* 1988:265-272.
25. Firoozabadi A. *Thermodynamics of Hydrocarbon Reservoirs*. New York, NY: McGraw-Hill; 1999.

Manuscript received Aug. 16, 2004, and revision received Apr. 28, 2005.